Science Advances
AAAS

advances.sciencemag.org/cgi/content/full/5/1/eaau7555/DC1

Supplementary Materials for

Rapid isotopic exchange in nanoparticles

Papri Chakraborty, Abhijit Nag, Ganapati Natarajan, Nayanika Bandyopadhyay, Ganesan Paramasivam, Manoj Kumar Panwar, Jaydeb Chakrabarti, Thalappil Pradeep*

*Corresponding author. Email: pradeep@iitm.ac.in

Published 4 January 2019, *Sci. Adv.* **5**, eaau7555 (2019)
DOI: 10.1126/sciadv.aau7555

This PDF file includes:

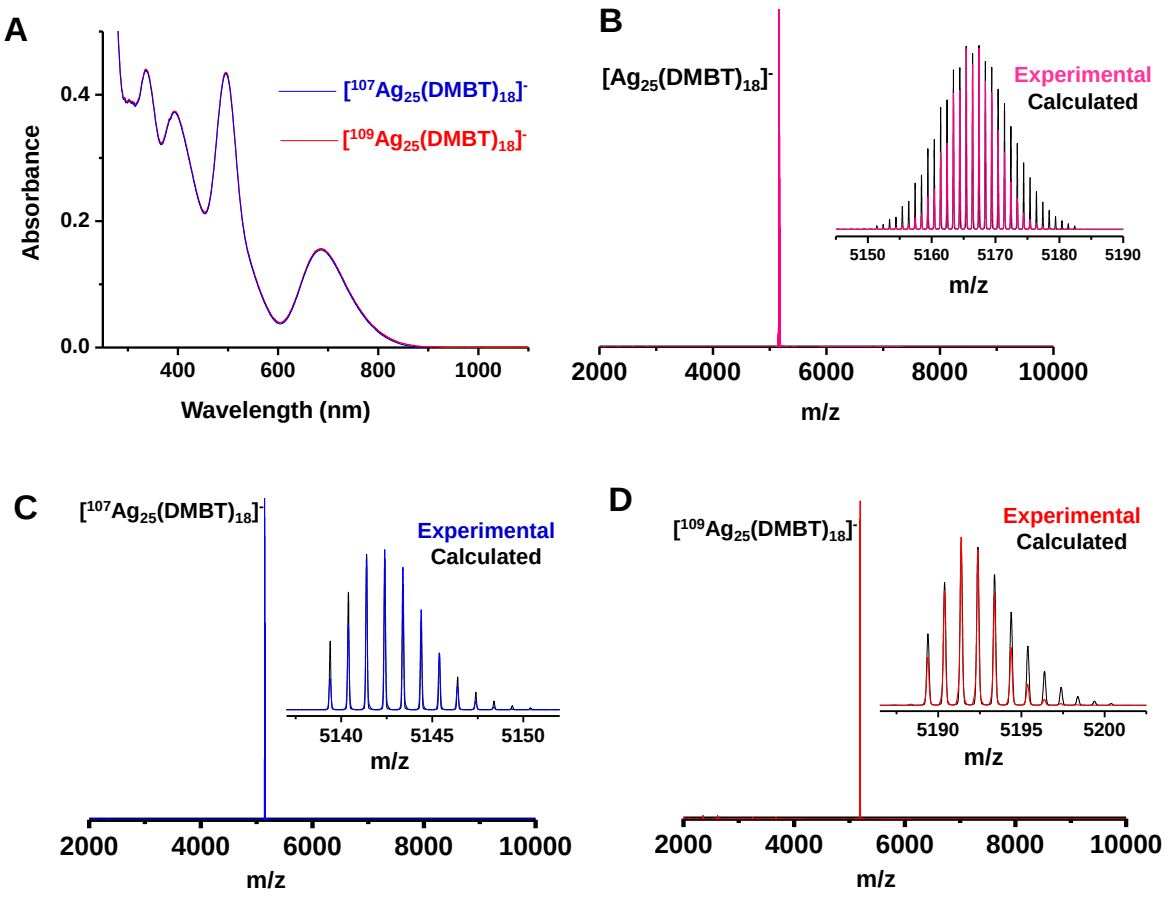

Fig. S1. Characterization of isotopically pure $[^{107}Ag_{25}(DMBT)_{18}]^-$ and $[^{109}Ag_{25}(DMBT)_{18}]^-$ clusters. (**A**) UV-vis spectra of $[^{107}Ag_{25}(DMBT)_{18}]^-$ and $[^{109}Ag_{25}(DMBT)_{18}]^-$ clusters showing identical features. ESI MS of (**B**) $[Ag_{25}(DMBT)_{18}]^-$ made from natural Ag, (**C**) $[^{107}Ag_{25}(DMBT)_{18}]^-$ and (**D**) $[^{109}Ag_{25}(DMBT)_{18}]^-$. Insets show the comparison of the experimental and calculated isotope patterns of the peaks. The minor differences in the experimental spectra (in **C** and **D**) in comparison to the calculated spectra are due to the slight contribution of the other isotope in each sample as the isotope enrichment was 98%.

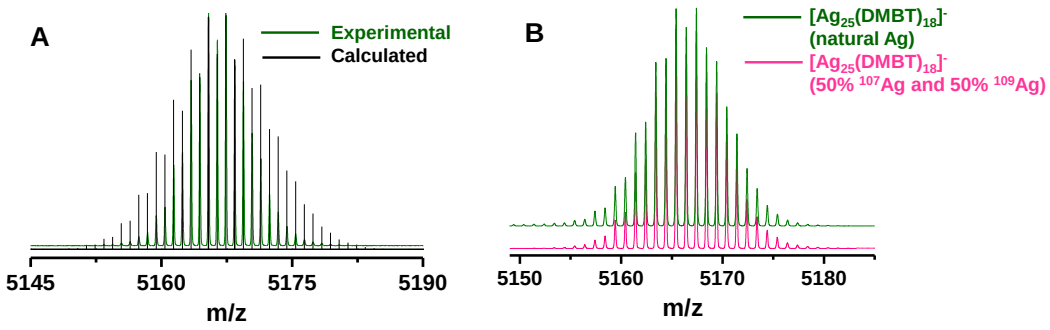

Fig. S2. Isotope patterns of the product obtained by reaction of $[^{107}Ag_{25}(DMBT)_{18}]^-$ and $[^{109}Ag_{25}(DMBT)_{18}]^-$ at 1:1 molar ratio. Experimental isotope distribution of the product obtained by mixing $[^{107}Ag_{25}(DMBT)_{18}]^-$ and $[^{109}Ag_{25}(DMBT)_{18}]^-$ at 1:1 molar ratio. The isotope pattern is compared with (**A**) the distribution computed considering 50% abundance of each isotope in $[Ag_{25}(DMBT)_{18}]^-$ and (**B**) experimental isotope patterns of $[Ag_{25}(DMBT)_{18}]^-$ synthesized from natural Ag.

N.B. In this case, the overall isotope distribution has contribution from the isotopes of the metal Ag and also C, H and S in the ligands. For the two parent clusters (Fig. 1 and S1) which are isotopically pure there is only one isotope of Ag. However, the product, which is a 1:1 mixture of the two isotopic clusters, has an isotope abundance of ^{107}Ag: ½ and ^{109}Ag: ½ and the isotope pattern for Ag will follow the binomial distribution and as a result will be broader compared to the monoisotopic case. This contribution from the isotopic abundance of Ag will be reflected in the overall isotope distribution and thus the product distribution is obviously broader than the two parent clusters.

Moreover natural abundance of Ag is ^{107}Ag (51.84%) and ^{109}Ag (48.16%). Hence the ratio of their abundances is 1.08, i.e. ~1, hence product distribution is similar to the cluster made of naturally abundant Ag.

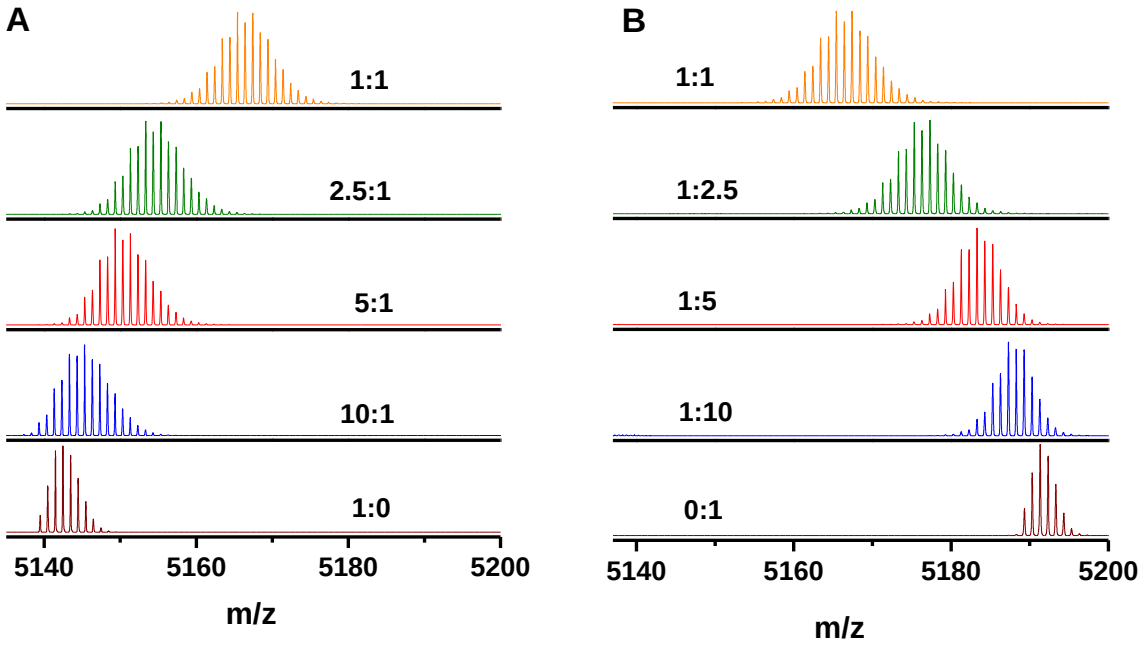

Fig. S3. ESI MS of reaction product obtained by mixing the two isotopic $[^{107}Ag_{25}(DMBT)_{18}]^-$ and $[^{109}Ag_{25}(DMBT)_{18}]^-$ clusters at various molar ratios. Product obtained by mixing $[^{107}Ag_{25}(DMBT)_{18}]^-$ and $[^{109}Ag_{25}(DMBT)_{18}]^-$ at varying molar ratios where in (**A**) $[^{107}Ag_{25}(DMBT)_{18}]^-$ cluster is kept in higher concentration and in (**B**) $[^{109}Ag_{25}(DMBT)_{18}]^-$ cluster is kept in higher concentration. The initial molar ratio of mixing the two clusters ($[^{107}Ag_{25}(DMBT)_{18}]^-$: $[^{109}Ag_{25}(DMBT)_{18}]^-$) is indicated for each product observed.

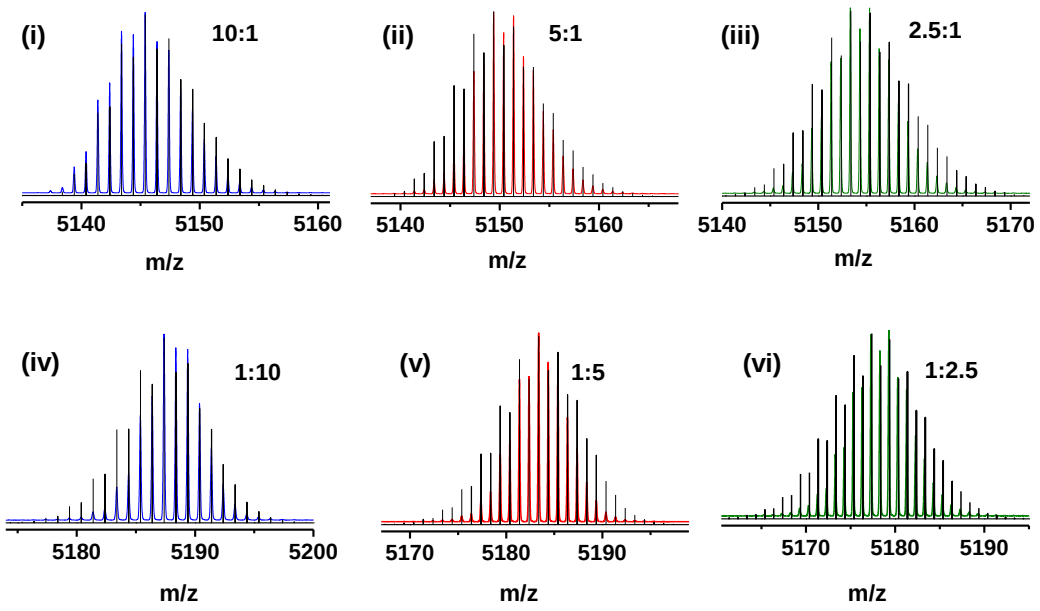

Fig. S4. Comparison of the experimental and calculated isotope patterns of the products obtained by mixing $[^{107}Ag_{25}(DMBT)_{18}]^-$ and $[^{109}Ag_{25}(DMBT)_{18}]^-$ at various molar ratios. Comparison of the experimental isotope patterns of the products obtained at different molar ratios of mixing the two isotopic clusters ($[^{107}Ag_{25}(DMBT)_{18}]^-$:$[^{109}Ag_{25}(DMBT)_{18}]^-$) with the calculated patterns. The experimental patterns showed best match with the calculated patterns considering the abundances of each isotope in the cluster from their initial molar ratio of mixing.

Note. Molar ratio of mixing ($[^{107}Ag_{25}(DMBT)_{18}]^-$: $[^{109}Ag_{25}(DMBT)_{18}]^-$) = x:y

Table S1. Abundance of ^{107}Ag in product = $\{x/(x + y)\} \times 100$ and ^{109}Ag in product = $\{y/(x + y)\} \times 100$.

Sl. No.	x:y	Abundance (^{107}Ag:^{109}Ag)	Sl. No.	x:y	Abundance (^{107}Ag:^{109}Ag)
1	10:1	90.909:9.091	5	1:10	9.091:90.909
2	5:1	83.333:16.667	6	1:5	16.667:83.333
3	2.5:1	71.428:28.571	7	1:2.5	28.571:71.428
4	1:1	50:50	8	1:1	50:50

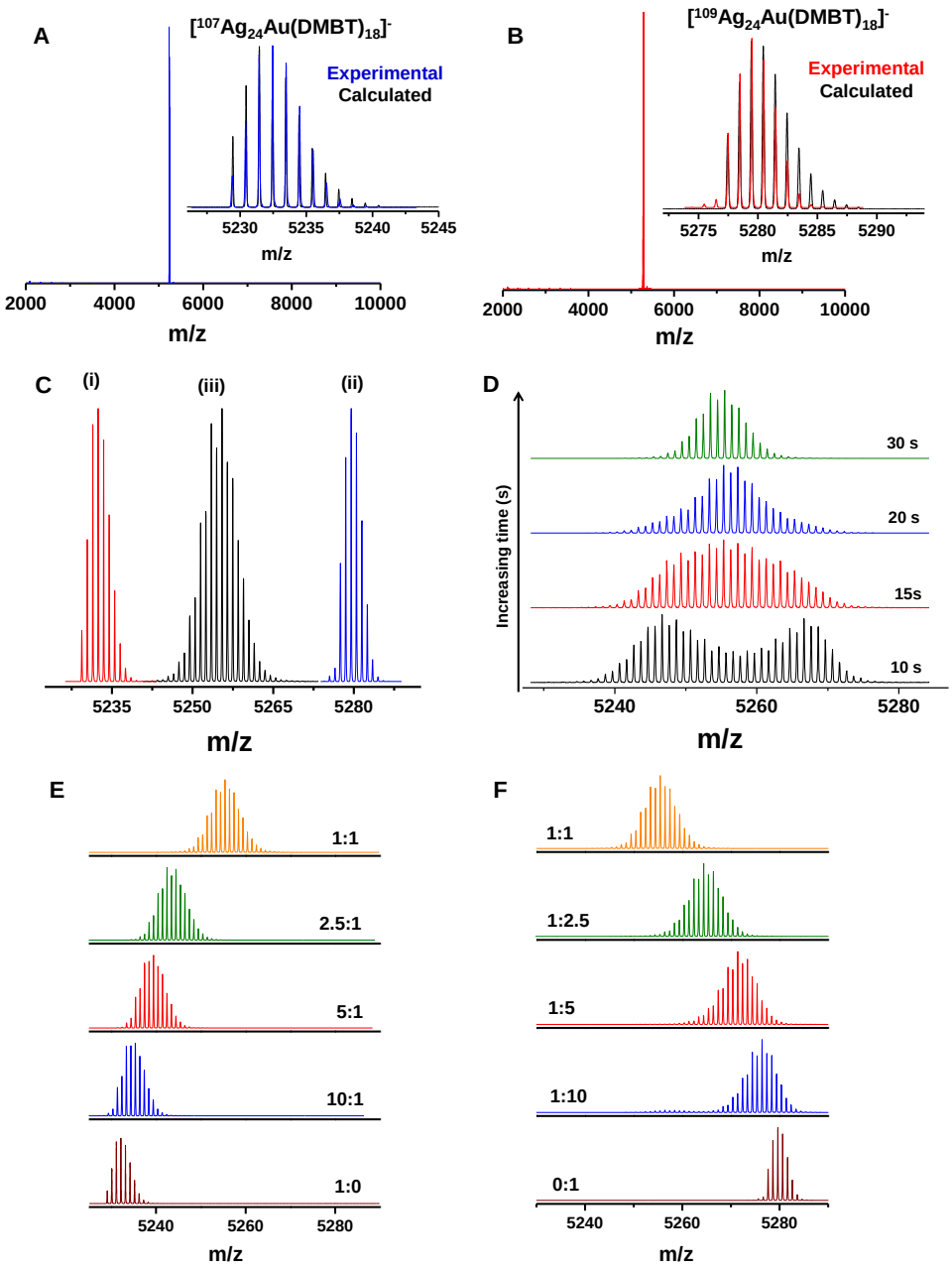

Fig. S5. Isotope exchange in $[Ag_{24}Au(DMBT)_{18}]^-$ clusters. ESI MS of (**A**) $[^{107}Ag_{24}Au(DMBT)_{18}]^-$ and (**B**) $[^{109}Ag_{24}Au(DMBT)_{18}]^-$. Insets show the comparison of the experimental and calculated isotope patterns. (**C**) Reaction of $[^{107}Ag_{24}Au(DMBT)_{18}]^-$ and $[^{109}Ag_{24}Au(DMBT)_{18}]^-$ in 1:1 molar ratio at room temperature, where (i), (ii) and (iii) denotes ESI MS of $[^{107}Ag_{24}Au(DMBT)_{18}]^-$, $[^{109}Ag_{24}Au(DMBT)_{18}]^-$ and the product (50% abundance of each isotope), respectively. All the spectra are shown in the same scale. (**D**) Intermediates stages of reaction in 1:1 molar ratio at -20 ^oC. (**E**) and (**F**) Reaction at various molar ratios, $[^{107}Ag_{24}Au(DMBT)_{18}]^-$: $[^{109}Ag_{24}Au(DMBT)_{18}]^-$ ratio is indicated in the figure.

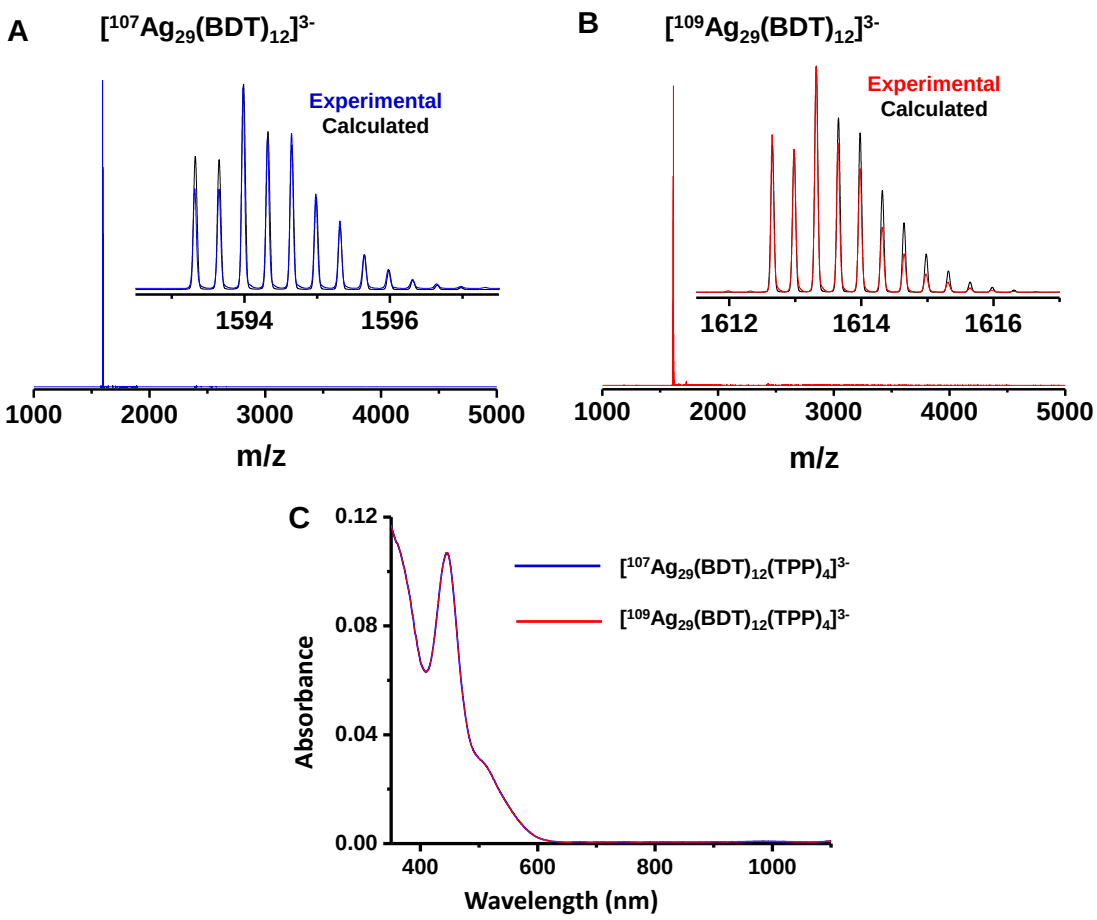

Fig. S6. Characterization of isotopically pure $[^{107}Ag_{29}(BDT)_{12}(TPP)_4]^{3-}$ and $[^{109}Ag_{29}(BDT)_{12}(TPP)_4]^{3-}$ clusters. ESI MS of (**A**) $[^{107}Ag_{29}(BDT)_{12}]^{3-}$ and (**B**) $[^{109}Ag_{29}(BDT)_{12}]^{3-}$ clusters. The labile TPP ligands were lost during ionization. Insets show the comparison of the experimental and calculated isotope patterns of the peaks. The minor differences in the experimental spectra in comparison to the calculated spectra are due to the slight contribution of the other isotope in each sample as the isotope enrichment was 98%. (**C**), UV-vis spectra of $[^{107}Ag_{29}(BDT)_{12}(TPP)_4]^{3-}$ and $[^{109}Ag_{29}(BDT)_{12}(TPP)_4]^{3-}$ clusters showing identical features.

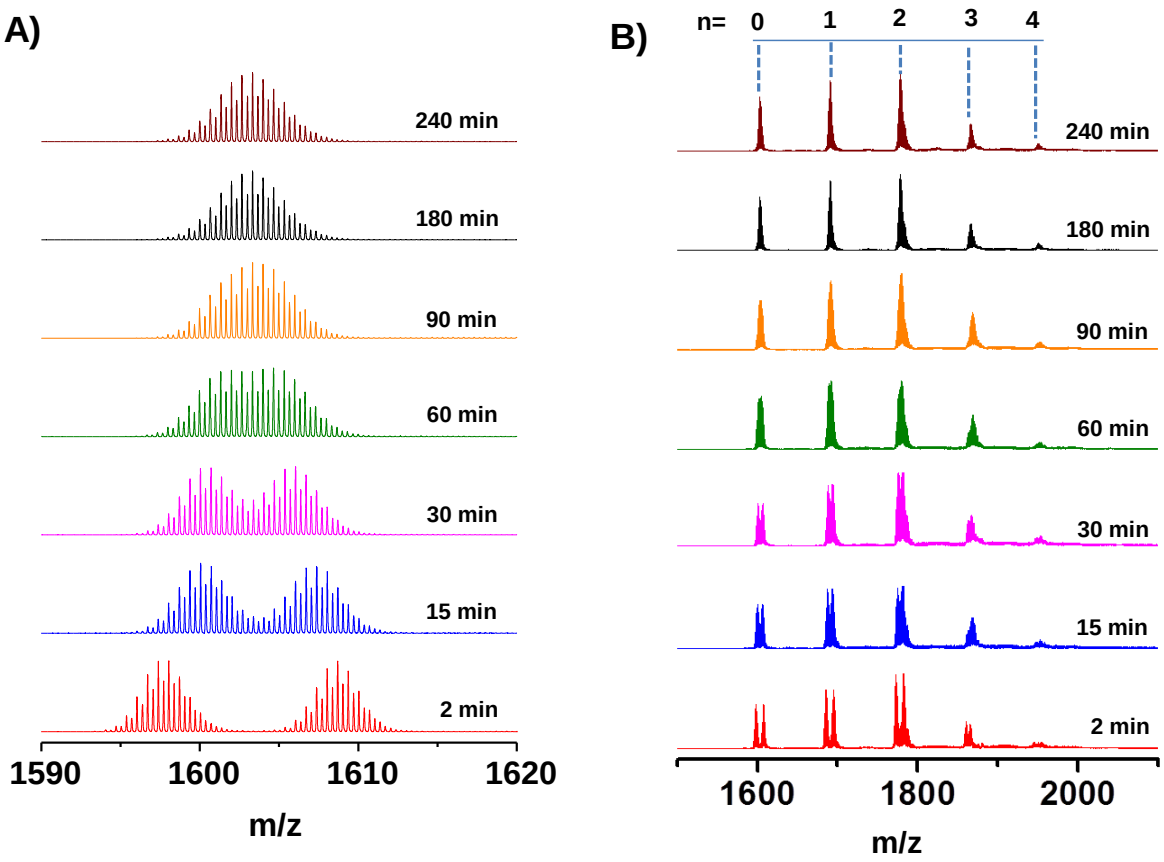

Fig. S7. Reaction between $[^{107}Ag_{29}(BDT)_{12}(TPP)_4]^{3-}$ and $[^{109}Ag_{29}(BDT)_{12}(TPP)_4]^{3-}$ clusters in 1:1 molar ratio at room temperature. (**A**) Intermediates stages of reaction between $[^{107}Ag_{29}(BDT)_{12}]^{3-}$ and $[^{109}Ag_{29}(BDT)_{12}]^{3-}$ in 1:1 molar ratio at room temperature. The mixture reaches equilibrium over a period of 2 h. (**B**) Intermediates stages of reaction between $[^{107}Ag_{29}(BDT)_{12}(TPP)_n]^{3-}$ (n=0-4) and $[^{109}Ag_{29}(BDT)_{12}(TPP)_n]^{3-}$ (n=0-4) in 1:1 molar ratio at room temperature, showing the intact TPP attached clusters in ESI MS. The mixture reaches equilibrium at similar time scales.

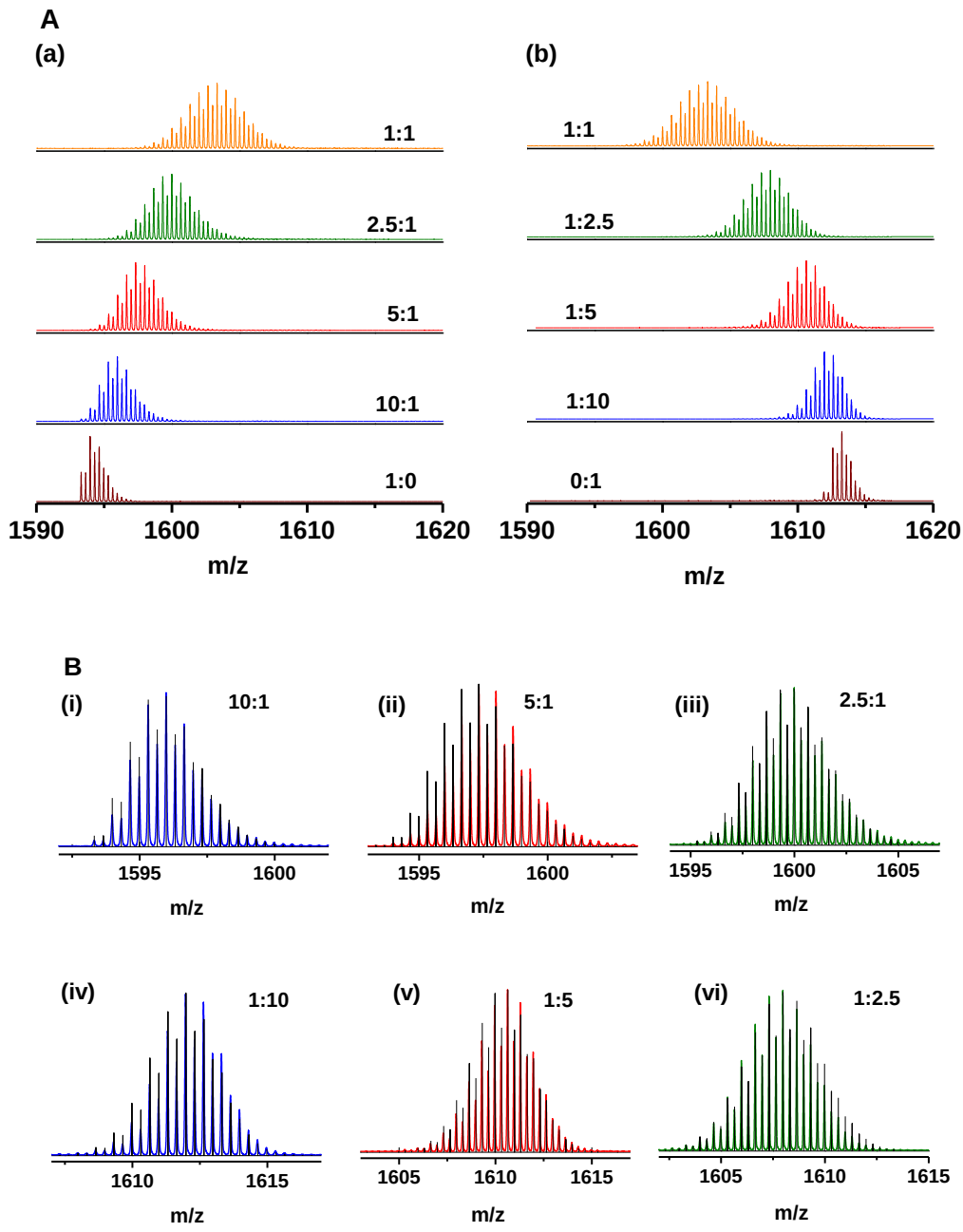

Fig. S8. ESI MS of reaction product obtained by mixing the two isotopic $[^{107}Ag_{29}(BDT)_{12}(TPP)_4]^{3-}$ and $[^{109}Ag_{29}(BDT)_{12}(TPP)_4]^{3-}$ clusters at various molar ratios. (**A**) Product obtained by mixing the two isotopic clusters $[^{107}Ag_{29}(BDT)_{12}]^{3-}$ and $[^{109}Ag_{29}(BDT)_{12}]^{3-}$ at varying molar ratios where in (**a**) $[^{107}Ag_{29}(BDT)_{12}]^{3-}$ is kept in higher concentration and in (**b**) $[^{109}Ag_{29}(BDT)_{12}]^{3-}$ is kept in higher concentration. The initial molar ratio of mixing the two clusters ($[^{107}Ag_{29}(BDT)_{12}]^{3-}$: $[^{109}Ag_{29}(BDT)_{12}]^{3-}$) is indicated for each product observed. (**B**) Comparison of the experimental isotope patterns of the products with the calculated isotope patterns considering the abundances of each isotope from their initial molar ratio of mixing.

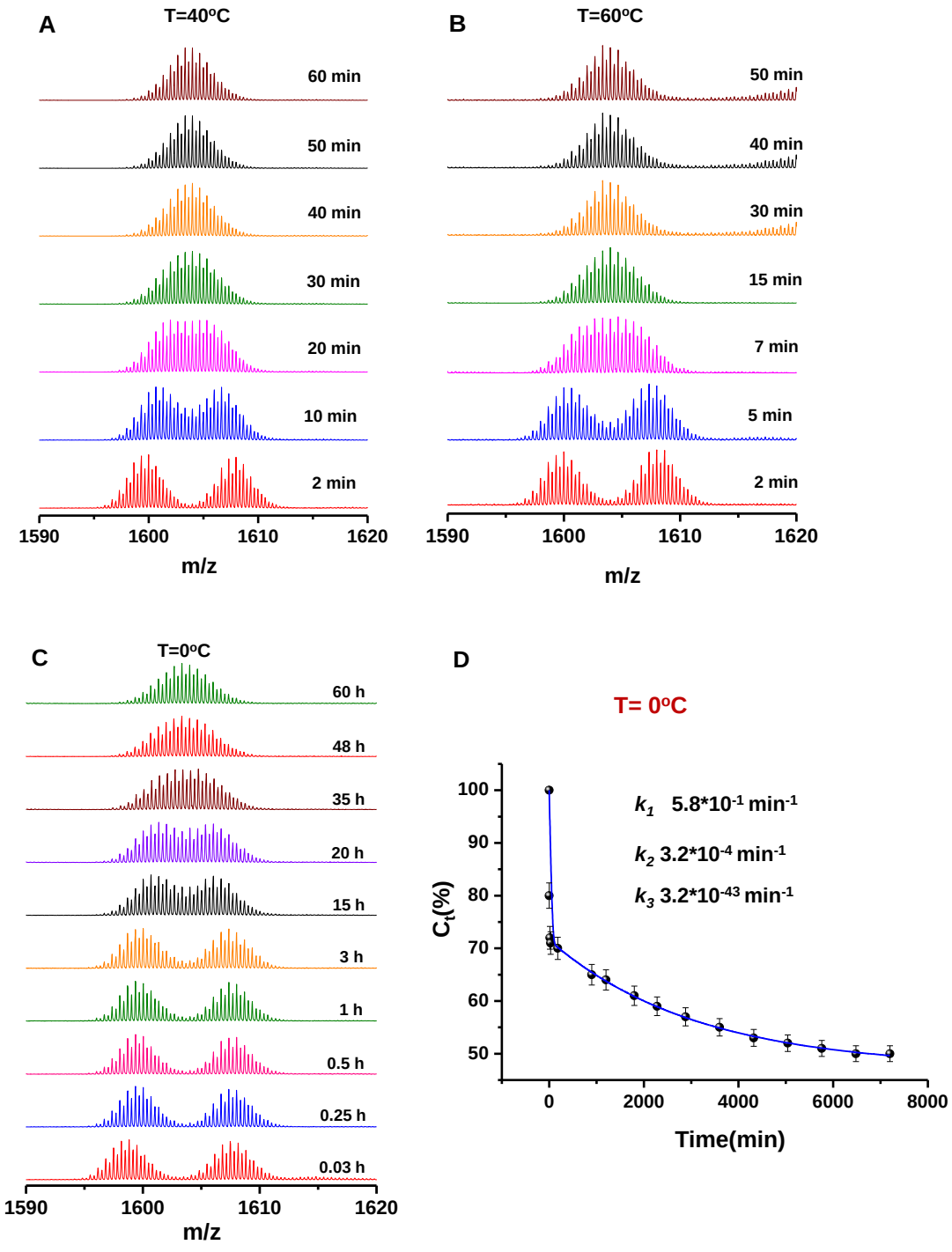

Fig. S9. Time-dependent study of reaction between $[^{107}Ag_{29}(BDT)_{12}(TPP)_4]^{3-}$ and $[^{109}Ag_{29}(BDT)_{12}(TPP)_4]^{3-}$ in 1:1 molar ratio at various temperatures. Time-dependent study showing the **i**ntermediates stages of reaction between $[^{107}Ag_{29}(BDT)_{12}]^{3-}$ and $[^{109}Ag_{29}(BDT)_{12}]^{3-}$ in 1:1 molar ratio at (**A**) 40 ^{o}C, (**B**) 60 ^{o}C and (**C**) 0 ^{o}C. (**D**) Kinetic plot of the percentage of un-exchanged parent cluster (C_t) versus time at 0^{o}C. The rate constants obtained from tri-exponential fitting are indicated in the figure.

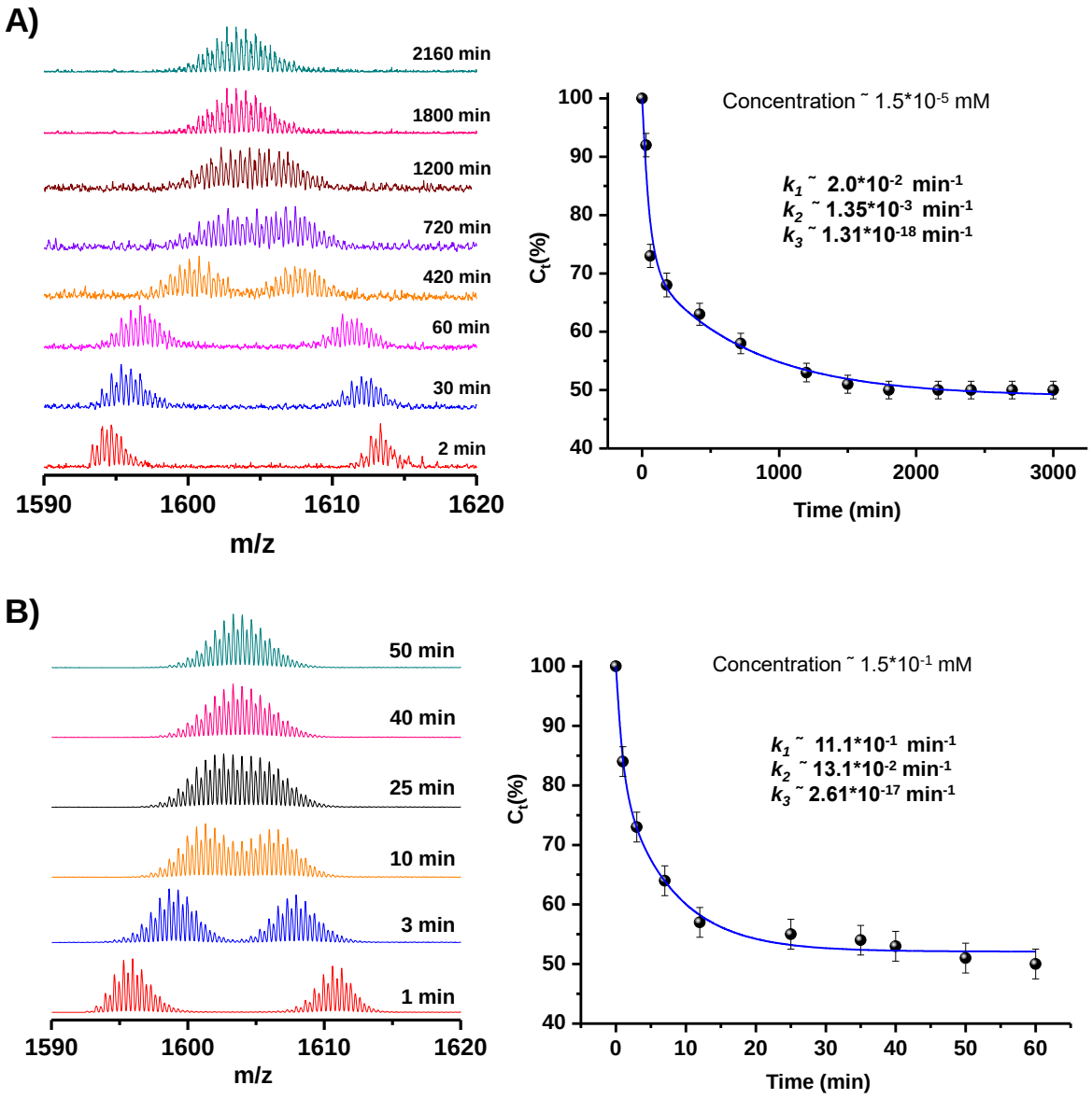

Fig. S10. Kinetic study of isotopic exchange at different concentrations of $[Ag_{29}(BDT)_{12}(TPP)_4]^{3-}$ clusters. Time-dependent ESI MS and corresponding kinetic study showing the rate constants of the reaction at **A**) $1.5*10^{-5}$ mM and **B**) $1.5*10^{-1}$ mM concentration.

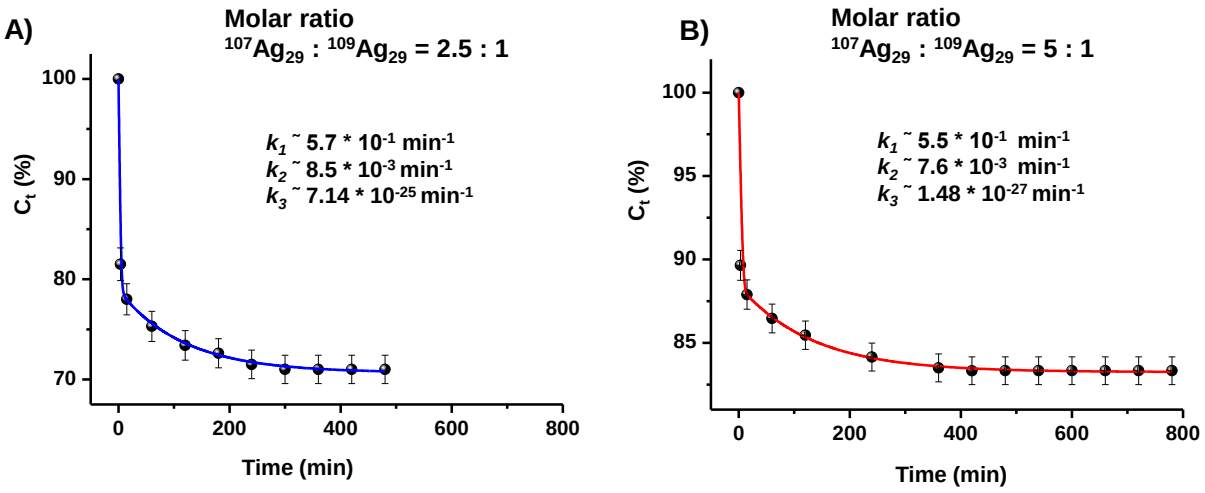

Fig. S11. Kinetic study of isotopic exchange in $[Ag_{29}(BDT)_{12}(TPP)_4]^{3-}$ clusters at different molar ratios of mixing. Kinetic study of isotopic exchange at molar ratios of mixing of $^{107}Ag_{29}$:$^{109}Ag_{29}$ clusters, (**A**) 2.5:1 and (**B**) 5:1. The rate constants of the three stages of exchange in each case are denoted in the figure.

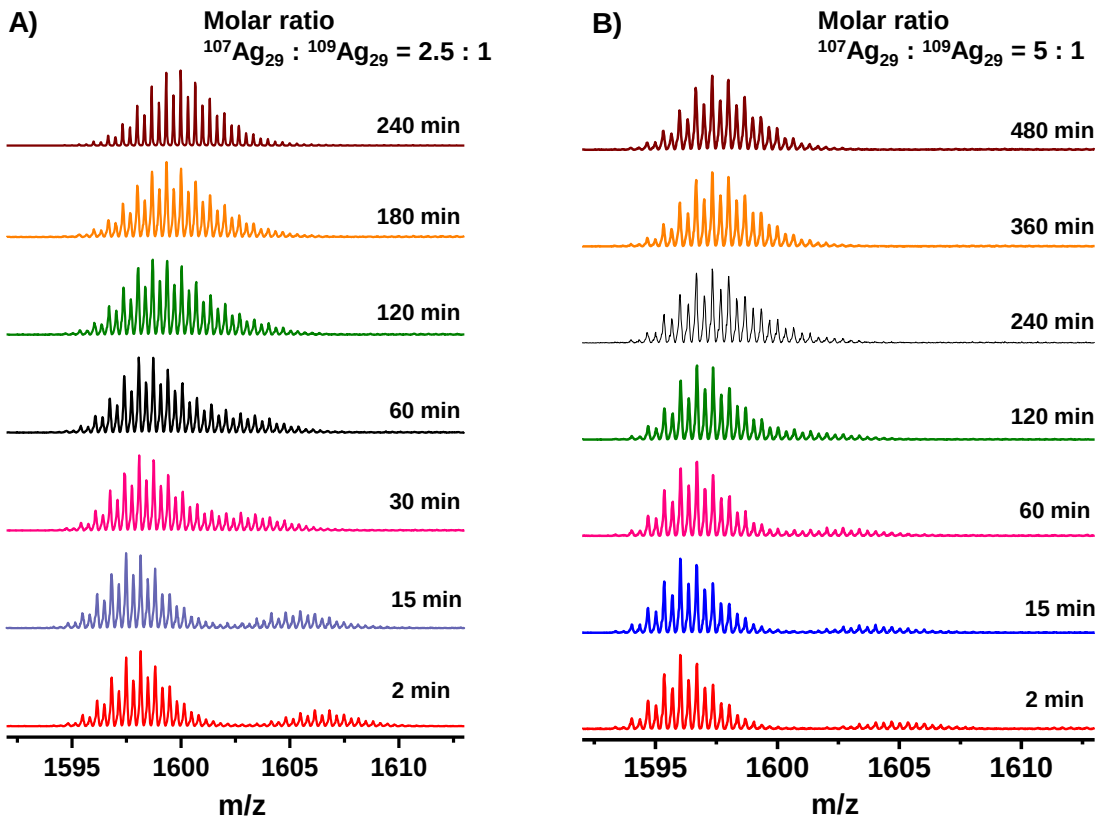

Fig. S12. Time-dependent study of reaction between $[^{107}Ag_{29}(BDT)_{12}(TPP)_4]^{3-}$ and $[^{109}Ag_{29}(BDT)_{12}(TPP)_4]^{3-}$ at various molar ratios. Time-dependent study showing the intermediate stages of reaction at $^{107}Ag_{29}$:$^{109}Ag_{29}$ molar ratios of (**A**) 2.5:1 and (**B**) 5:1.

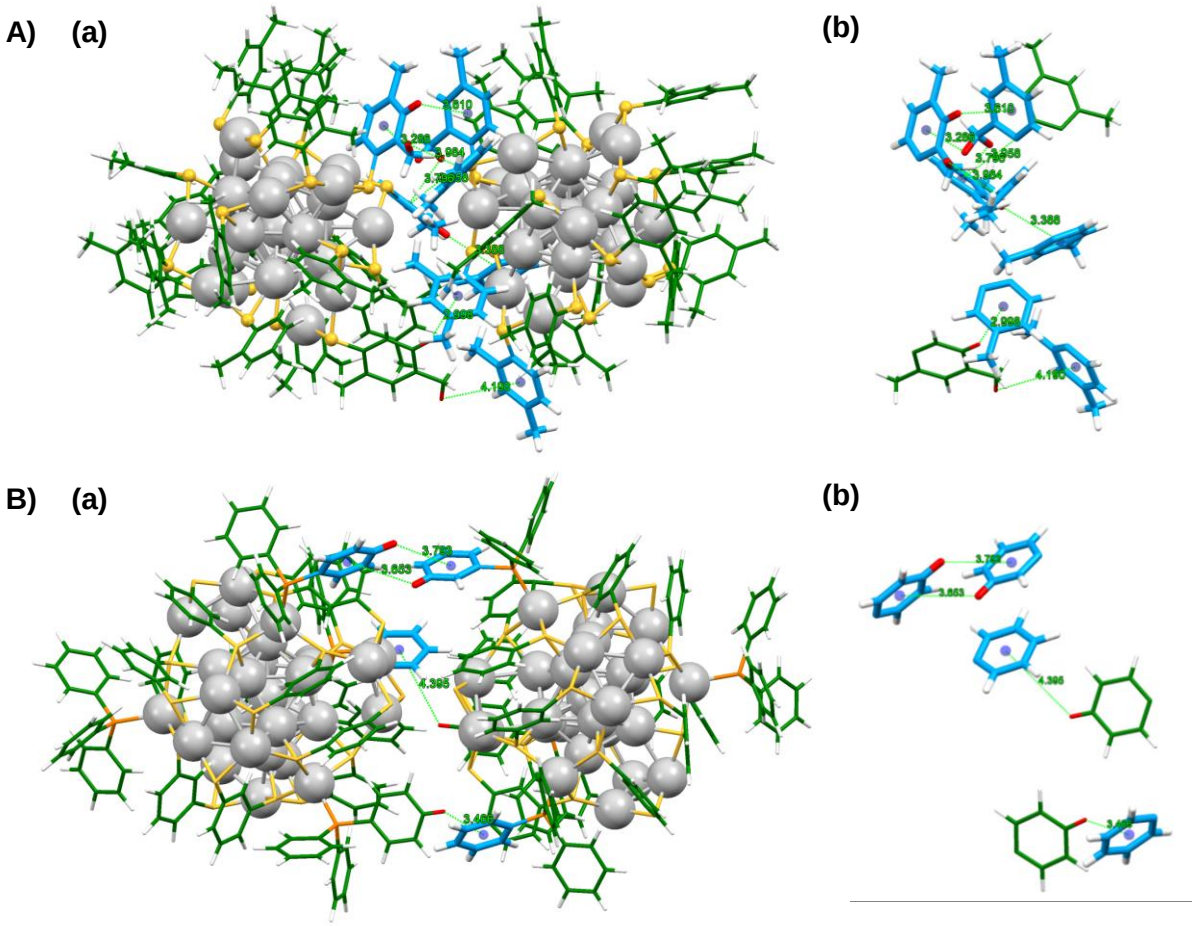

Fig. S13. Molecular docking studies. Lowest energy geometry obtained from docking two **A**) $[Ag_{25}(DMBT)_{18}]^-$ and **B**) $[Ag_{29}(BDT)_{12}(TPP)_4]^{3-}$ clusters. C-H···π interactions are indicated in the figure. Color codes: grey: Ag, yellow: S, orange: P, green: ligands. The H atoms involved in these interactions are shown in red and the benzene rings involved are shown in blue. Expanded view of the ligands involved in these C-H···π interactions are shown in the insets b.

Table S2. Table showing ZPE and Gibbs free energy (*G*) values of the isotopic clusters.

(a) For $[Ag_{29}(BDT)_{12}(TPP)_4]^{3-}$ clusters

(i) Isotopically pure reactants

Cluster	ZPE (eV)	G (eV)
$[^{107}Ag_{29}(BDT)_{12}(TPP)_4]^{3-}$	2.400	-1262.250
$[^{109}Ag_{29}(BDT)_{12}(TPP)_4]^{3-}$	2.394	-1262.271

(ii) Mixed isotope product clusters with composition (m,n) = (15,14) and (14,15) in $[^{107}Ag_m{}^{109}Ag_n(BDT)_{12}(TPP)_4]^{3-}$.

(m.n) = (15,14)				(m.n) = (14,15)			
Position of ^{107}Ag atoms	Position of ^{109}Ag atoms	ZPE (eV)	G (eV)	Position of ^{107}Ag atoms	Position of ^{109}Ag atoms	ZPE (eV)	G (eV)
C-1 I-12 S-2	S-14	2.397	-1262.260	S-14	C-1 I-12 S-2	2.397	-1262.261
S-15	C-1 I-12 S-1	2.397	-1262.260	C-1 I-12 S-1	S-15	2.397	-1262.261
C-1 I-6 S-8	I-6 S-8	2.397	-1262.260	I-6 S-8	C-1 I-6 S-8	2.397	-1262.261

(b) For $[Ag_{25}(DMBT)_{18}]^-$ clusters

(i) Isotopically pure reactants

Cluster	Zero-point energy (ZPE) (eV)	Free Energy (G) (eV)
$[^{107}Ag_{25}(DMBT)_{18}]^-$	1.655	-502.919
$[^{109}Ag_{25}(DMBT)_{18}]^-$	1.650	-502.938

(ii) Mixed isotope product clusters with composition (m,n) = (13,12) and (12,13) in $[^{107}Ag_m{}^{109}Ag_n(DMBT)_{18}]^-$

(m.n) = (13,12)				(m.n) = (12,13)			
Position of ^{107}Ag atoms	Position of ^{109}Ag atoms	ZPE (eV)	G (eV)	Position of ^{107}Ag atoms	Position of ^{109}Ag atoms	ZPE (eV)	G (eV)
C-1 I-12	S-12	1.652	-502.928	S-12	C-1 I-12	1.652	-502.929
S-12 C/I-1	C/I-12	1.652	-502.928	C/I-12	S-12 C/I-1	1.652	-502.929
C-1 I-6 S-6	I-6 S-6	1.652	-502.928	I-6 S-6	C-1 I-6 S-6	1.652	-502.929

N.B. C, I and S refers to centre, icosahedron and staple positions, respectively.